

Innovative Trajectory Planning of a Marker Robot on Steel Coils and Slabs

Mohammad Sajjad Mahdiah*

Department of Mechanical Engineering,
Shahid Chamran University of Ahvaz, Ahvaz, Iran
E-mail: s.mahdiah@scu.ac.ir

*Corresponding author

Received: 16 April 2024, Revised: 24 September 2024, Accepted: 2 November 2024

Abstract: Writing on steel coils and slabs (to mark them) is one of the problems faced by domestic steelmaking industries. Currently, this operation is done with the help of human power, which has its own drawbacks. In order to solve these problems, a marker robot is supposed to be applied. This robot writes letters, numbers, and signs on steel coils with an automatic paint spray gun. The robot intended for this purpose is a 5 degrees of freedom robot (5DOF), 3 degrees of freedom are related to the robot arm, and the other 2 degrees are related to the robot wrist. Due to the special conditions governing the problem, the solution of inverse kinematics has been done by the geometric method, which is simpler than the algebraic method. In order to determine the path of the robot (the path of letters and numbers), a series of time-dependent Equations have been applied. To show the accuracy of the planned trajectory, simulations have been carried out on the mentioned robot and the movement trajectory of the end-effector and the configuration of the arm have been graphically displayed. The programming of the robot's trajectory has been performed in MATLAB and LabVIEW and Visual Nastran has been applied to simulate the robot's trajectory.

Keywords: Innovative Solution, Inverse Kinematics, Marker Robot, Steel Coils and Slabs, Trajectory Planning

Biographical notes: **Mohammad Sajjad Mahdiah** received his PhD in Mechanical Engineering from the University of Tehran, Iran in 2016. He is currently an Assistant Professor at the Department of Mechanical Engineering, Shahid Chamran University of Ahvaz, Iran. His research areas are inverse engineering, 3D printing, and metal forming.

Research paper

COPYRIGHTS

© 2025 by the authors. Licensee Islamic Azad University Isfahan Branch. This article is an open access article distributed under the terms and conditions of the Creative Commons Attribution 4.0 International (CC BY 4.0)

(<https://creativecommons.org/licenses/by/4.0/>)



1 INTRODUCTION

In today's world industry, the use of robots in different parts of the production line is increasing [1-4]. For example, applying different kinds of robots is a privilege in steel factories [5-6]. An example of these robots is the writer (or marker) robot, which draws letters, numbers, and symbols on steel coils and slabs using a mobile automatic paint spray (pistol) [7-8]. Carrying out such proportional movements requires the proper design of the path of the robot's end-effector. In 1991, "Su" and his colleagues presented an effective and optimal method for designing the trajectory of paint-spraying robots, which was used in the future. Designing a suitable trajectory for paint spraying robots was a vital thing in the industry at that time because it prevented the wastage of a significant amount of paint, resulting in a significant saving in time and cost [9]. In addition, the final stage of the design of the robot requires several analytical and numerical methods such as finite element methods [10-14]. In 1994, Antonio conducted research on the design of the movement trajectory of a robot that covered different parts by spraying and obtained results. The research conducted by Antonio was the foundation of the next industrial projects [15]. In 1997, Asakawa developed a new method of designing the trajectory of car body paint spraying robots. His method, which was implemented under the title of Teachingless robots, was successful and saved time and money for the Hyundai company [16]. In 1996, Hertling conducted research on the design of complex and curved paths of the paint-spraying robot. Of course, Hertling's work remained a research project, but his research was very valuable for subsequent research [17]. To truly manufacture the marker robot, several precise manufacturing and production methods such as forming and machining should be applied [18-27]. Currently, in the steel industries of our country, writing on the steel coils and slabs is done by human power, which has its own problems. Therefore, according to the domestic industry's need for such robots, a research plan was defined, and the results related to the trajectory planning of the robot arm are presented in this article. According to the parameters and characteristics of the designed robot, it is necessary to first solve the direct and inverse kinematics of the problem in order to obtain the transformation matrix of the joints. Next, the trajectory planning of the robot to write letters is done, and position-time Equations of the path of writing letters are extracted. After obtaining the Equations of the path, the angles of each joint during the operation of writing letters are obtained with the help of programming in MATLAB and LabVIEW. In the end, the result of the simulation was done by Visual Nastran software.

2 RESEARCH METHOD

2.1. Solving Inverse Kinematics for Writing on Slabs

In order to determine the transformation matrix of the joints, the parameters of the Denavit-Hartenberg robot according to "Fig. 1" are given in "Table 1" [28].

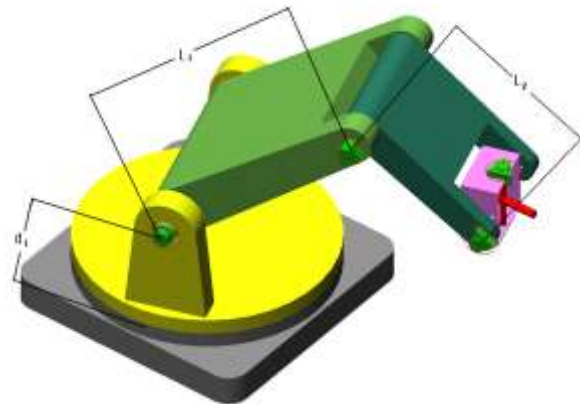


Fig. 1 Schematic view of the robot and its parameters.

Table 1 Denavit-Hartenberg parameters of the robot

i	α_{i-1}	a_{i-1}	d_i	θ_i
1	0	0	d_1	θ_1
2	-90	0	0	θ_2
3	0	L_1	0	θ_3
4	0	L_2	0	θ_4
5	90	0	0	θ_5

The frameworks considered to solve the problem according to "Fig. 2" are the basic framework (O), the final end-effector framework (EE), and the panel framework (S). The frame of the painting is mounted on a stationary slab.

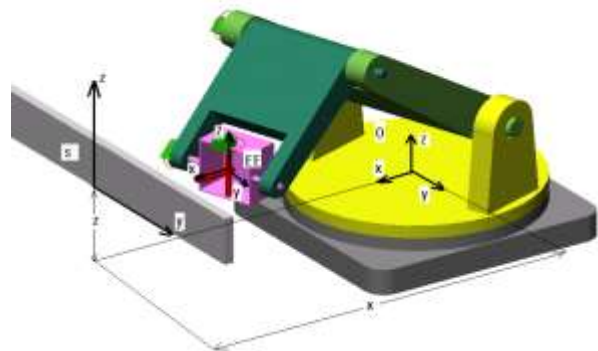


Fig. 2 Display of the basic frameworks, the EF, and the slab.

Thus, the relationship between the transformation matrices of the frames is according to Equation (1):

$${}^0T_E = {}^0T_S {}^ST_E \quad (1)$$

The transformation matrix of the end-effector relative to the base of the robot is equal to 0T_E . The matrix 0T_5 is obtained by multiplying the transformation matrices 1 to 5 (according to Equation (2)).

$${}^0T_5 = {}^0T_1 {}^1T_2 {}^2T_3 {}^3T_4 {}^4T_5 \quad (2)$$

Finally, the matrix 0T_E can also be expressed according to Equation (3):

$${}^0T_E = \begin{bmatrix} 1 & 0 & 0 & px \\ 0 & 1 & 0 & py \\ 0 & 0 & 1 & pz \\ 0 & 0 & 0 & 1 \end{bmatrix} \quad (3)$$

The pistol should be perpendicular to the table while writing, however, the part related to the transformation matrix 0T_E is equal to the identity matrix [29].

px , py , pz are the final positions of the robot's end-effector from the base, which is explained in the trajectory planning section 2-3. As stated, due to the special conditions governing the problem, the geometric method has been used to obtain the inverse kinematics of the robot. The special condition of the problem is the verticality of the robot's end-effector on the table, which must be maintained at all times.

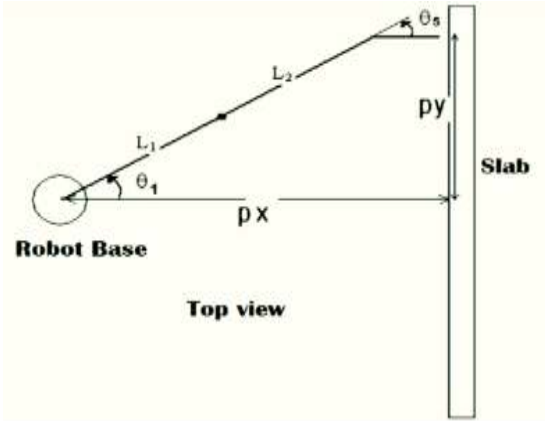


Fig. 3 Robot top view for expressing θ_1 and θ_5 .

According to the explanations provided, the method of obtaining the angles from θ_1 to θ_5 has been examined in the following. As it is clear from "Fig. 3", θ_1 and θ_5 are obtained from Equations (4 and 5):

$$\theta_1 = \tan^{-1}(py/px) \quad (4)$$

$$\theta_5 = -\tan^{-1}(py/px) = -\theta_1 \quad (5)$$

It should be noted that since the conventional rotation directions of θ_1 and θ_5 are opposite to each other, so their signs are also opposite.

According to "Fig. 4", θ_3 is obtained from Equation (6):

$$\begin{aligned} w^2 &= pz^2 + (px/\cos\theta_1)^2 \\ w^2 &= L_1^2 + L_2^2 + 2L_1L_2\cos(\pi - \theta_3) \\ \Rightarrow \theta_3 &= \cos^{-1}\left(\frac{pz^2 + (px/\cos\theta_1)^2 - L_1^2 - L_2^2}{2L_1L_2}\right) \end{aligned} \quad (6)$$

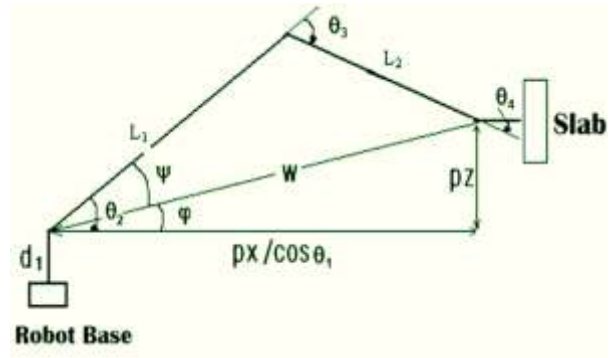


Fig. 4 View of the robot to express θ_2 , θ_3 and θ_4 .

Also, θ_2 is obtained as Equation (7) after the following calculations:

$$\begin{aligned} \theta_2 &= -\psi - \varphi \\ \varphi &= \tan^{-1}\left(\frac{pz}{px/\cos\theta_1}\right) \\ \frac{L_2}{\sin\psi} &= \frac{L_1}{\sin\alpha} = \frac{w}{\sin(\pi - \theta_3)} \\ \psi &= \sin^{-1}\left(\frac{L_2 \sin(\pi - \theta_3)}{\sqrt{pz^2 + (px/\cos\theta_1)^2}}\right) \\ \Rightarrow \theta_2 &= -\sin^{-1}\left(\frac{L_2 \sin(\pi - \theta_3)}{\sqrt{pz^2 + (px/\cos\theta_1)^2}}\right) - \tan^{-1}\left(\frac{pz}{px/\cos\theta_1}\right) \end{aligned} \quad (7)$$

And according to "Fig. 4", θ_4 is obtained according to Equation (8):

$$\theta_4 = -\theta_2 - \theta_3 \quad (8)$$

2.2. Solving Inverse Kinematics for Writing on Coils

The parameters of Denavit Hartenberg are similar to "Table 1". In this way, it is possible to obtain the transformation matrix of the joints in relation to each

other. For example, below (Equation (9)) is the transformation matrix of the third joint compared to the second:

$${}^2T_3 = \begin{bmatrix} \cos(\theta_3) & -\sin(\theta_3) & 0 & L_1 \\ \sin(\theta_3) & \cos(\theta_3) & 0 & 0 \\ 0 & 0 & 1 & 0 \\ 0 & 0 & 0 & 1 \end{bmatrix} \quad (9)$$

The frameworks considered to solve the problem according to “Fig. 5” are the basic framework (0), the end-effector framework (EE), and the panel framework (S). The panel frame is mounted on the coil.

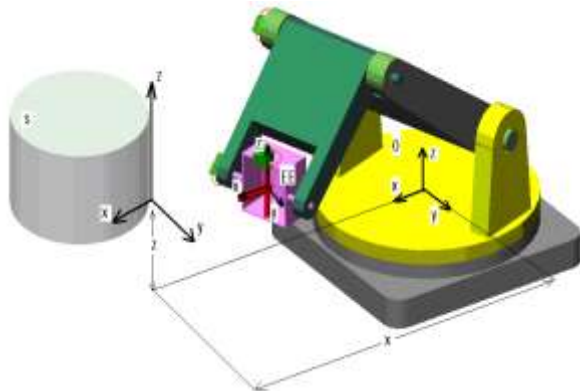


Fig. 5 Display of the basic frameworks, the end-effector, and the panel (coil).

The paint pistol should be perpendicular to the coil when writing. Therefore, due to the special status of the project, the geometric method has been used to obtain the inverse kinematics of the robot. The special condition of the problem is the verticality of the robot’s end-effector on the coil, which must be maintained at every moment. With the explanations provided, the angles θ_1 to θ_5 can be obtained in the following order. As it is clear from “Fig. 6”, θ_1 is obtained from Equations (10 and 11):

$$\begin{aligned} \theta_1 &= \tan^{-1}(k / px) \\ k &= R \sin \alpha \\ px &= X + x(t) \end{aligned} \quad (10)$$

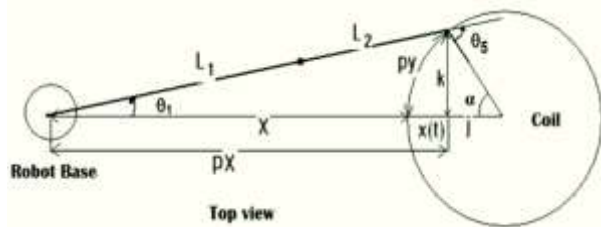


Fig. 6 The top view of the robot to express θ_1 and θ_5 .

Where, R is the radius of the coil and X is the longitudinal distance of the coil from the base of the robot (“Fig. 6”).

$$\begin{aligned} \theta_1 &= \tan^{-1}(R \sin \alpha / px) \\ \alpha &= py / R \end{aligned} \quad (11)$$

α is expressed in radians:

$$\Rightarrow \theta_1 = \tan^{-1}\left(\frac{R \sin(py / R)}{px}\right) \quad (12)$$

According to “Fig. 6”, θ_5 is obtained from Equations (13):

$$\begin{aligned} \theta_5 &= -\theta_1 - \alpha \\ \alpha &= py / R \\ \Rightarrow \theta_5 &= -[R - R \cos(py / R) + py / R] \end{aligned} \quad (13)$$

$\theta_2, \theta_3,$ and θ_4 are the same as writing on the slabs:

$$\theta_3 = \cos^{-1}\left(\frac{pz^2 + (px / \cos \theta_1)^2 - L_1^2 - L_2^2}{2L_1L_2}\right) \quad (14)$$

$$\theta_2 = -\sin^{-1}\left(\frac{L_2 \sin(\pi - \theta_3)}{\sqrt{pz^2 + (px / \cos \theta_1)^2}}\right) - \tan^{-1}\left(\frac{pz}{px / \cos \theta_1}\right) \quad (15)$$

$$\theta_4 = -\theta_2 - \theta_3 \quad (16)$$

2.3. Trajectory Planning

A reference point (0,0) is determined for each letter, and the movement starts from this point and ends at this point. As mentioned, due to the use of an automatic paint spray gun (automatic change of disconnecting and connecting action), there is no need for the final operator to move away from the keyboard anymore, and the letters are written continuously, therefore, its complete path should be considered for each letter. Thus, it starts from the reference point and includes all the components of the letters as well as the interface between the components. Finally, it returns to the reference point. For example, according to “Fig. 7”, to write the letter E, eight lines should be used, four of which are main (2, 3, 5, 7) and four are auxiliary (1, 4, 6, and 8). The paint spray gun is on when crossing the main lines (solid lines) and off when crossing the auxiliary lines (pale lines). Also, the path of the letter C is also shown, in which segments 1 and 3 are auxiliary and arc 2 is main.

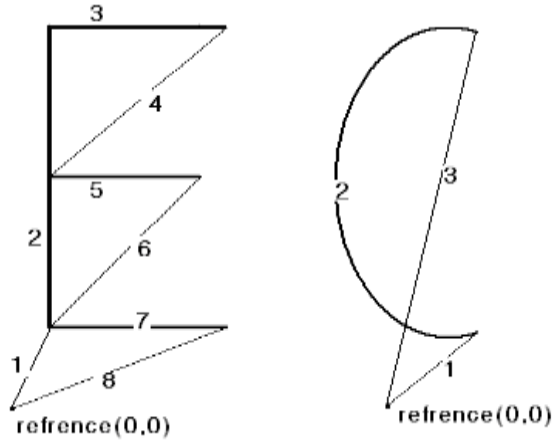


Fig. 7 The moving path of letters E and C.

The path of other letters is obtained similarly. Now the Equations of the lines and curves forming each letter or number should be written as locus Equations. For example, the Equations of the first three-line segments of the letter E are in the form of Equation (17):

$$\begin{cases} z = -0.2857y \\ z = 20 \\ y = -10 \end{cases} \quad (17)$$

Also, polar coordinates should be used to write the Equations of circular or ellipse components of letters. For example, the Equation of the elliptical arc of the letter C is given in Equation (18):

$$\begin{cases} y = 50 \sin \theta - 60 \\ z = 80 \cos \theta + 100 \\ -0.54\pi \leq \theta \leq 0.54\pi \end{cases} \quad (18)$$

Now the Equations that are in terms of locus should be converted into locus-time Equations. This work is achieved according to the speed of the robot's performers and its acceleration time. For example, the Equation of the first line segment of the letter E in terms of time is according to Equation (19):

$$\begin{cases} y(t) = -48.0762t \\ z(t) = 13.735t \\ 0 \leq t \leq 1.456 \end{cases} \quad (19)$$

Also, the Equation of the elliptical arc of the letter C in terms of time is according to Equation (20):

$$\begin{cases} \theta = -0.4727t + 3.9611 \\ y(t) = 80 \cos \theta + 100 \\ z(t) = 50 \sin \theta - 60 \\ 1.46 \leq t \leq 8.46 \end{cases} \quad (20)$$

Thus, the values of px , py , and pz used in the transformation matrix are according to Equation (21):

$$\begin{cases} px = X \\ py = 300 + y(t) \\ pz = Z + z(t) \end{cases} \quad (21)$$

Where, X and Z are the longitudinal distance and height of the board/panel from the base of the robot. For example, in order to write on the slab, the transformation matrix 0T_E for the first segment of the letter E is as Equation (22):

$${}^0T_E = \begin{bmatrix} 1 & 0 & 0 & X \\ 0 & 1 & 0 & 300 - 48.0862t \\ 0 & 0 & 1 & 13.735t + Z \\ 0 & 0 & 0 & 1 \end{bmatrix} \quad (22)$$

For writing on the coils, $x(t)$ according to "Fig. 8" is obtained as Equation (23):

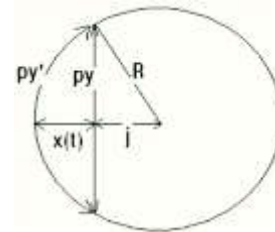


Fig. 8 The conversion of a flat panel to a circular panel (coil).

$$\begin{aligned} x(t) &= R - j \\ j &= R \cos \alpha \\ x(t) &= R - R \cos \alpha \\ \alpha &= py / R \\ \Rightarrow x(t) &= R - R \cos(py / R) \end{aligned} \quad (23)$$

For example, the 0T_E conversion matrix for the first segment of the letter E is according to Equation (24):

$${}^0T_E = \begin{bmatrix} 1 & 0 & 0 & X + R - R \cos((300 - 28.086t) / R) \\ 0 & 1 & 0 & 300 - 48.0862t \\ 0 & 0 & 1 & 13.735t + Z \\ 0 & 0 & 0 & 1 \end{bmatrix} \quad (24)$$

3 SIMULATION AND RESULTS

3.1. Simulations for Writing on Steel Slabs

The inverse kinematics programming of the robot is done in MATLAB software, whose inputs are six letters or numbers and robot parameters such as the length of the members and the distance from the base of the robot and the output of the robot angles program, which is obtained from the inverse kinematics solution. The angles obtained from the output of the program can be checked by the direct kinematic Equations of the robot, which are shown in “Fig. 9” of the related diagrams.

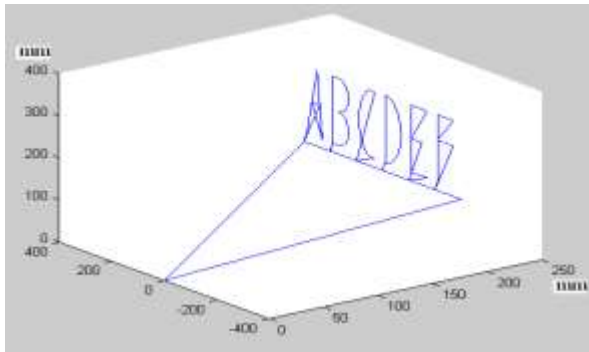


Fig. 9 Testing the program for writing on the slab.

Simulink and Visual Nastran software have been used to simulate the robot's movement path. Figure 10 shows the model designed in Simulink for kinematic simulation [30].

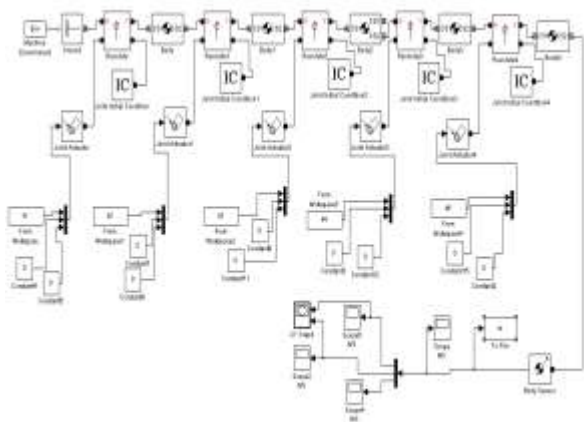


Fig. 10 Model designed in Simulink.

Also, in “Fig. 11”, two states of the machine (robot arm system) simulated for the designed model are shown. The simulated machine follows the trajectory of the given letters.

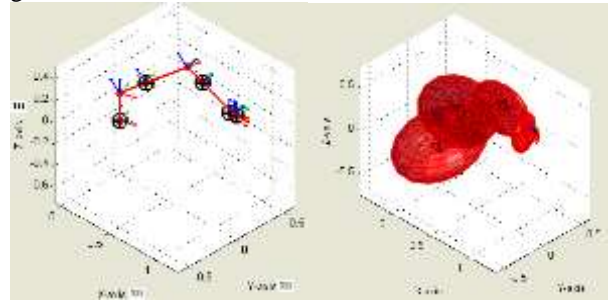


Fig. 11 Two states of the machine simulated for the designed model.

According to the simulation performed in Simulink, the final position is obtained in terms of two y-z axes, whose diagram is shown in “Fig. 12”.

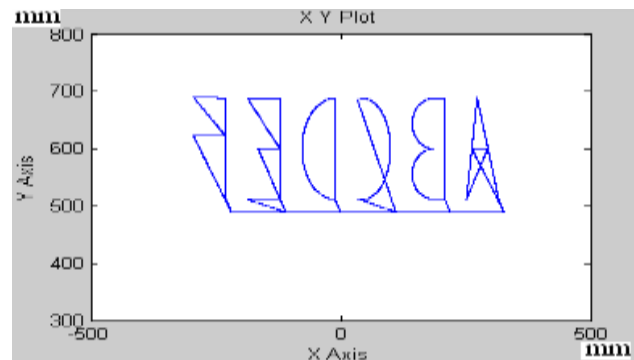


Fig. 12 Position of the end-effector.

In fact, “Fig. 12” shows the verification of the simulation results with Simulink because the end-effector has exactly followed the path of the desired letters. Nastran is a powerful simulation software that provides reliable results. Figure 13 shows four states of the robot in the simulation operation in Visual Nastran.

As it is clear from “Fig. 13”, the robot follows the path of the letters exactly, and this means the accuracy of the path design and solving the inverse kinematics problem. Also, according to “Fig. 13”, it is evident that the end-effector of the robot is perpendicular to the slab at any moment. As a result, the spray gun is perpendicular to the surface of the slab at any moment, and this causes

the dispersion of the paint from the gun to be minimized and the best quality of the written text is achieved.



Fig. 13 Different states of the robot during the simulation operation.

3.2. Simulations for Writing on Steel Coils

The inverse kinematics programming of the robot is done in MATLAB software, whose inputs are six letters or numbers and robot parameters such as the length of the links, the distance of the coil from the base of the robot, the radius of the coil, and the output of the robot angles program, which is obtained from solving the inverse kinematics. The angles obtained from the output of the program can be tested by direct kinematic Equations of the robot, which are shown in “Fig. 14” of the program test diagram.

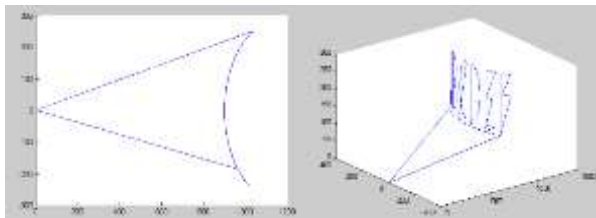


Fig. 14 Testing the program for writing on the coil.

As it is clear from “Fig. 14”, the path of the end-effector is located on the arc of the circle that corresponds to the circumference of the steel coil. Also, “Fig. 15” shows the Block Diagram view of the program written in LabVIEW software.

Similar to the program written in MATLAB, it takes 6 letters or numbers as input, and according to the parameters of the robot set in the Block Diagram, the angles of the robot obtained from the kinematics solution save the results obtained as output in the corresponding files. Figure 16 shows the Front panel view of the written program after its execution. As it is known, the proposed test diagram is completely consistent with the test diagram drawn in MATLAB.

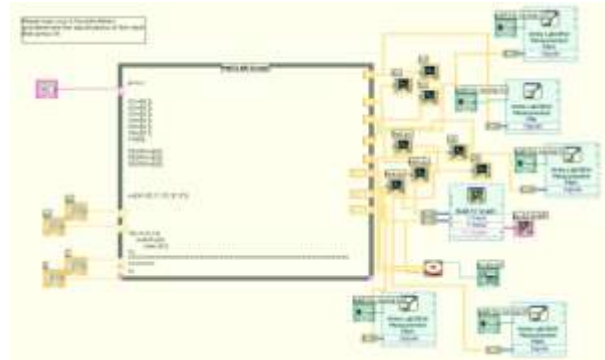


Fig. 15 The block diagram view of the program written in LabVIEW.

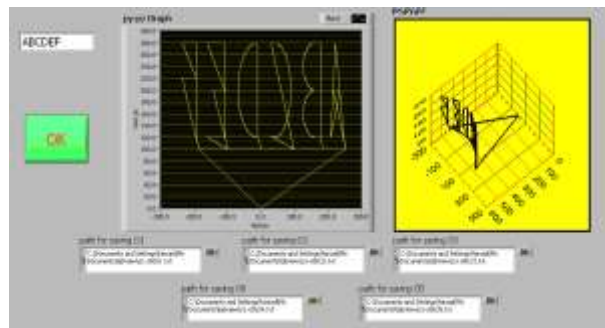


Fig. 16 Front panel view of the executed program.

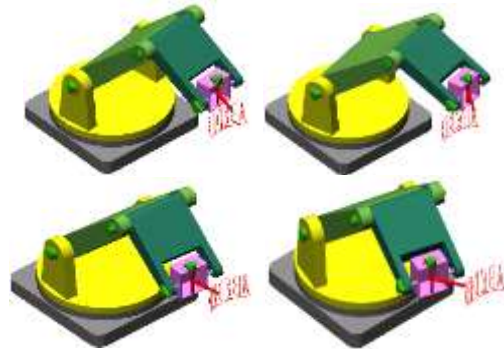


Fig. 17 Different states of the robot while writing on the coil.

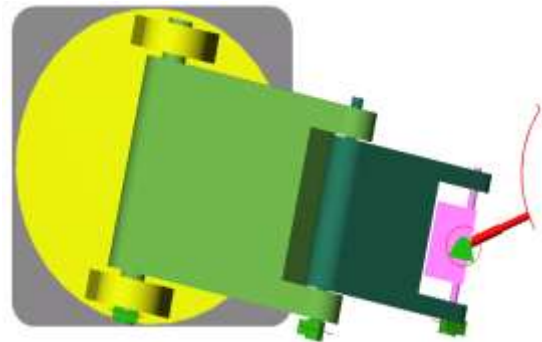


Fig. 18 The view from the top of the robot after the end of the simulation.

In addition, Visual Nastran software has been used to simulate the movement of the robot. Figure 17 shows the four states of the robot during the simulation operation, as well as the top view of the robot after the end of the simulation operation is shown in “Fig. 18” in the Visual Nastran software.

As it is clear from “Figs. 17 and 18”, the end-effector is perpendicular to the coil at any moment, and the path of writing the letters is circular and in line with the body of the coil, and this indicates the verification of solving the problem.

4 CONCLUSIONS

The goal of this article was to design the path of the robot designed for marking on the steel slabs and coils, which obtained the following results:

1- The first step to achieve this goal is the direct kinematics solution of the problem, which was done after determining the robot's Denavit-Hartenberg parameters and then the matrices Joint transformation was obtained.

2- Due to the special conditions governing the problem, the inverse kinematics of the robot was performed using the geometric method, which is much simpler and more reliable than the algebraic method.

3- Designing the path of the robot was done with the help of designing the path of the letters and the required angles of the joints were extracted during the operation.

4- Finally, the verification of solving the problem was ensured by carrying out simulation operations with strong and reliable software such as Nastran and LabVIEW.

ACKNOWLEDGMENTS

We are grateful to the Research Council of Shahid Chamran University of Ahvaz for financial support (SCU.EM1403.39184).

REFERENCES

- [1] Goel, R., Gupta, P., Robotics and Industry 4.0, A Roadmap to Industry 4.0: Smart Production, Sharp Business and Sustainable Development, 2020, pp. 157-169.
- [2] Day, C. P., Robotics in Industry—Their Role in Intelligent Manufacturing, Engineering, Vol. 4, No. 4, 2018, pp. 440-445.
- [3] Bragança, S., et al., A Brief Overview of the Use of Collaborative Robots in Industry 4.0: Human Role and Safety, in Occupational and Environmental Safety and Health, P.M. Arezes, et al., Editors, Springer International Publishing: Cham., 2019, pp. 641-650.
- [4] Tantawi, K. H., Sokolov, A., and Tantawi, O., Advances in Industrial Robotics: From Industry 3.0 Automation to Industry 4.0 Collaboration. in 2019 4th Technology Innovation Management and Engineering Science International Conference (TIMES-iCON), 2019.
- [5] Javaid, M., et al., Substantial Capabilities of Robotics in Enhancing Industry 4.0 Implementation. Cognitive Robotics, Vol. 1, 2021, pp. 58-75.
- [6] Kerber, E., et al. Towards Robotic Fabrication in Joining of Steel, In ISARC, Proceedings of the International Symposium on Automation and Robotics in Construction, IAARC Publications, 2018.
- [7] Crisnapati, P. N., et al., Pasang Aksara Bot: A Balinese Script Writing Robot Using Finite State Automata Transliteration Method, In Journal of Physics: Conference Series, IOP Publishing, 2019.
- [8] Meena, J., Kumar, T. S., and Amal, T., Design and Implementation of a Multi-Purpose End-Effector Tool for Industrial Robot, In 2021 International Symposium of Asian Control Association on Intelligent Robotics and Industrial Automation (IRIA), IEEE, 2021.
- [9] Suh, S. H., et al., A Prototype Integrated Robotic Painting System: Software and Hardware Development, In Proceedings of 1993 IEEE/RSJ International Conference on Intelligent Robots and Systems (IROS'93), IEEE, 1993.
- [10] Mahdieh, M. S., Esteki, M. R., Feasibility Investigation of Hydroforming of Dental Drill Body by FEM Simulation, Journal of Modern Processes in Manufacturing and Production, Vol. 11, No. 2, 2022, pp. 71-83.
- [11] Mahdieh, M. S., Monjezi, A., Investigation of an Innovative Cleaning Method for the Vertical Oil Storage Tank by FEM Simulation, Iranian Journal of Materials Forming, 2022.
- [12] Mahdieh, M. S., et al., A Study on Stamping of Airliner's Tail Connector Part Through FEM Simulation, Journal of Simulation and Analysis of Novel Technologies in Mechanical Engineering, 2023.
- [13] Mahdieh, M. S., Zadeh, H. M. B., and Reisabadi, A. Z., Improving Surface Roughness in Barrel Finishing Process Using Supervised Machine Learning, Journal of Simulation and Analysis of Novel Technologies in Mechanical Engineering, Vol. 15, No. 2, 2023, pp. 5-15.
- [14] Sajjad Mahdieh, M., Nazari, F., and Khairullah, A. R., A Study on The Effects of Different Pad Materials on Brake System Performance of a High-Capacity Elevator by FEM Simulation. International Journal of Advanced Design and Manufacturing Technology, Vol. 65, 4, 2024, pp. 61.
- [15] Antonio, J. K., Optimal Trajectory Planning for Spray Coating, In Proceedings of the 1994 IEEE International Conference on robotics and Automation, IEEE, 1994.

- [16] Asakawa, N., Takeuchi, Y., Teachingless Spray-Painting of Sculptured Surfaces by An Industrial Robot, In Proceedings of the International Conference on Robotics and Automation, IEEE, 1997.
- [17] Hertling, P., et al., Task Curve Planning for Painting Robots, Process Modeling and Calibration, IEEE Transactions on Robotics and Automation, Vol. 12, No. 2, 1996, pp. 324-330.
- [18] Mahdieh, M. S., The Surface Integrity of Ultra-Fine Grain Steel, Electrical Discharge Machined Using Iso-Pulse and Resistance-Capacitance-Type Generator, Proceedings of the Institution of Mechanical Engineers, Part L: Journal of Materials: Design and Applications, Vol. 234, No. 4, 2020, pp. 564-573.
- [19] Mahdieh, M. S., Recast Layer and Heat-Affected Zone Structure of Ultra-Fined Grained Low-Carbon Steel Machined by Electrical Discharge Machining. Proceedings of the Institution of Mechanical Engineers, Part B: Journal of Engineering Manufacture, Vol. 234, No. 5, 2020, pp. 933-944.
- [20] Mahdieh, M. S., Improving Surface Integrity of Electrical Discharge Machined Ultra-Fined Grain Al-2017 by Applying RC-Type Generator, Proceedings of the Institution of Mechanical Engineers, Part E: Journal of Process Mechanical Engineering, 2023, pp. 09544089231202329.
- [21] Mahdieh, M. S., Mahdavinejad, R., Comparative Study on Electrical Discharge Machining of Ultrafine-Grain Al, Cu, and Steel, Metallurgical and Materials Transactions A, Vol. 47, No. 12, 2016, pp. 6237-6247.
- [22] Mahdieh, M. S., Mahdavinejad, R., Recast Layer and Micro-Cracks in Electrical Discharge Machining of Ultra-Fine-Grained Aluminum, Proceedings of the Institution of Mechanical Engineers, Part B: Journal of Engineering Manufacture, Vol. 232, No. 3, 2018, pp. 428-437.
- [23] Mahdieh, M. S., Mahdavinejad, R. A., A Study of Stored Energy in Ultra-Fined Grained Aluminum Machined by Electrical Discharge Machining. Proceedings of the Institution of Mechanical Engineers, Part C: Journal of Mechanical Engineering Science, Vol. 231, No. 23, 2017, pp. 4470-4478.
- [24] Mahdieh, M. S., Zare-Reisabadi, S., Effects of Electro-Discharge Machining Process on Ultra-Fined Grain Copper, Proceedings of the Institution of Mechanical Engineers, Part C: Journal of Mechanical Engineering Science, Vol. 233, No. 15, 2019, pp. 5341-5349.
- [25] Saraeian, P., et al., Influence of Vibratory Finishing Process by Incorporating Abrasive Ceramics and Glassy Materials on Surface Roughness of CK45 Steel. ADMT Journal, Vol. 9, No. 4, 2016, pp. 1-6.
- [26] Vakili Sohrforozani, A., et al., A Study of Abrasive Media Effect on Deburring in Barrel Finishing Process, Journal of Modern Processes in Manufacturing and Production, Vol. 8, No. 3, 2019, pp. 27-39.
- [27] Vakili Sohrforozani, A., et al., Effects of Abrasive Media on Surface Roughness in Barrel Finishing Process, ADMT Journal, Vol. 13, No. 3, 2020 pp. 75-82.
- [28] Craig, J. J., Introduction to Robotics, Pearson Educacion, 2006.
- [29] Lewis, F., Mechanical Engineering Handbook Ed. Frank Kreith Boca Raton: CRC Press LLC, 1999.
- [30] Karris, S. T., Introduction to Simulink with Engineering Applications, Orchard Publications, 2006.